Design Methodology for a Hovering Disc with an Annular Air Curtain: Coupled Cushion-Ground Model and Pressure-Sealing Design Procedure

Fabio Vulpi, Ph.D.

27.10.2025

Abstract

We present a coupled modelling and design framework for a hovering disc supported by a central pressure cushion and an annular high-velocity air curtain that acts as a *dynamic pressure seal* (rather than a thrust source). The curtain suppresses radial leakage from the core, enabling a stable high-pressure region capable of supporting an external load. The coupled model comprises: (i) an axisymmetric, low-Mach core governed by an anisotropic Darcy reduction, and (ii) a momentum-based curtain sub-model applied as a mixed (Robin) sealing boundary. We provide a step-by-step computational procedure for implementation and sizing, including lift matching, leakage, a seal number, and power estimates. The method yields a clear, code-ready basis for performance assessment and dimensioning of air-cushion hover devices.

1 Geometry and Notation

The geometry follows Fig. 1, defining the coordinate system and characteristic dimensions:

- R_{tot} – total radius of the disc.
- h – hovering height from the ground.
- h_{eff} – effective sealing gap accounting for ground roughness, $h_{\text{eff}} = h - \varepsilon_g$.
- p_0 – ambient pressure; $p_c = W/(\pi R_{\text{tot}}^2)$ – cushion pressure supporting the load W.
- U_{out}, ρ_j – speed and density of the outer jet.
- μ – dynamic viscosity; R_g – specific gas constant for air.
- $\dot{m}_{\text{in}}$ – air mass flow entering internal region.
- $\dot{m}_{\text{out}}$ – air mass flow of outer region.
- $\dot{m}_{\text{loss}}$ – air mass flow exiting internal region.
- b_0 – slot thickness of the outer annular jet at injection; the jet centreline is located at $R^- = R_{\text{tot}} - b_0/2$.
- $b(z)$ – local width of the curtain slot as a function of z (constant or weakly varying).
- ε_g – representative ground roughness used to define the effective sealing gap $h_{\text{eff}} = h - \varepsilon_g$.
- Assumptions: $b_0 \ll R_{\text{tot}}$, axisymmetric mean flow, low-Re in the cushion.

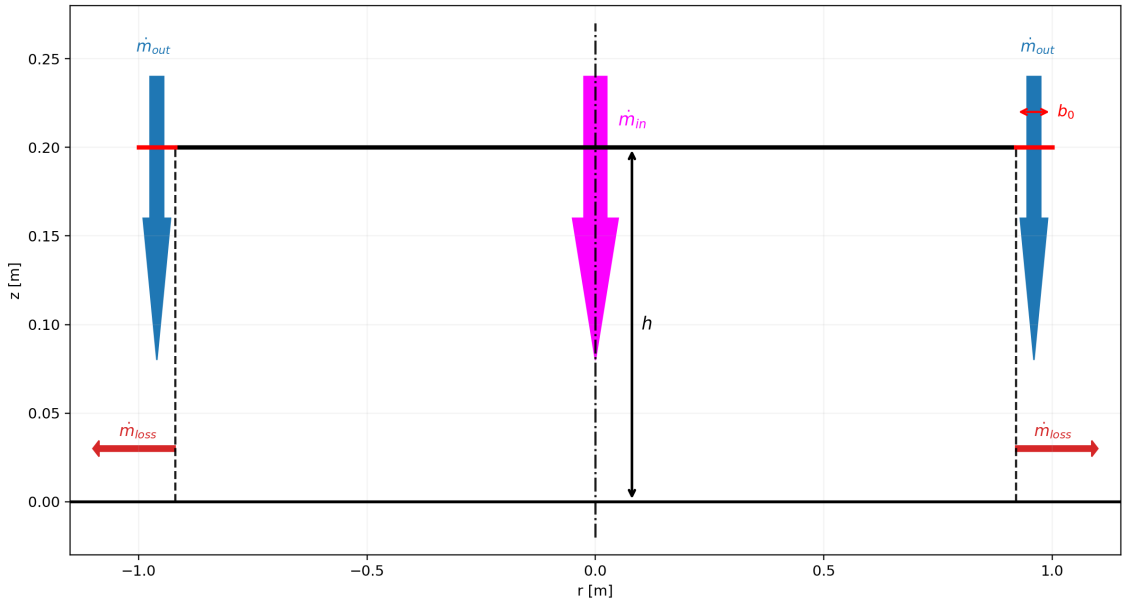

Figure 1 – Schematic of the hovering disc with two concentric jets: the outer annular curtain and the central make-up flow.

Table 1 – Default model parameters and empirical coefficients (nominal values are exemplary and require calibration).

Symbol	Description	Unit	Nominal value
α_r	Radial permeability coefficient	—	(e.g. 0.1)
α_z	Axial permeability coefficient	—	(e.g. 0.05)
E	Entrainment coefficient (wall-jet)	—	(e.g. 0.3)
C_f	Wall friction coefficient	—	(e.g. 0.005)
k_e	Wall-jet thickness growth rate	m/m	(e.g. 0.01)
K_{turn}	Momentum loss coefficient at turning	—	(e.g. 1.2)
$D_{m,\min}$	Minimum deflection modulus	—	(e.g. 0.2)

2 Model Overview

The cushion region ($0 \le r \le R^-$, $0 \le z \le h$) contains the pressurized air responsible for lift generation. Under isothermal, low–Mach conditions the mean flow obeys an *anisotropic Darcy–Brinkman* law:

$$u = -\frac{\kappa_r}{\mu}\,\partial_r p, \qquad w = -\frac{\kappa_z}{\mu}\,\partial_z p, \tag{1}$$

where $\kappa_r = \alpha_r h^2$ and $\kappa_z = \alpha_z h^2$ represent effective permeabilities in the radial and vertical directions. Inertia is neglected provided $Re_c = \rho U_c h/\mu \ll 1$; if this limit is exceeded, a Brinkman correction may be added (outside the present scope). Mass conservation and state equation read

$$\frac{1}{r}\,\partial_r(r\rho u) + \partial_z(\rho w) = 0, \qquad p = \rho R_g T_0, \tag{2}$$

under the isothermal assumption $T = T_0$.

3 Simulation Methodology

This section presents a clear, step-by-step procedure for simulating the coupled dynamics of the core cushion region and the outer annular curtain jet. The algorithm is designed to determine

the steady pressure and velocity fields in both regions, and thereby to compute the load-carrying capacity, leakage mass flows, and power requirement of the hover system.

1. Domains and coupling overview

The hover disc system is conceptually split into two interacting regions:

- The *core cavity*, defined by $0 \le r \le R^-$, $0 \le z \le h$, filled with pressurized air that supports the load and from which a peripheral leakage ring allows outflow.
- The *outer-jet region*, comprising the annular slot at $r = R^-$ through which the high-velocity curtain issues downward, impinges on the ground, and subsequently transitions into a radial wall-jet along the ground surface.

The key coupling mechanism is as follows: the outer jet impinges, creating a rim pressure distribution $p_{\text{edge}}(z)$ at the boundary $r = R^-$; this rim pressure acts as a boundary condition for the core pressure field. In turn, the core pressure field determines the leakage mass flux and thus affects the required outer jet flow and velocity to maintain equilibrium.

2. Governing sub-problems

2.1 Outer jet / curtain model Given a trial outer-slot exit velocity U_{out} and mass flow $\dot{m}_{\text{out}}$, the outer-jet sub-model now uses:

- The prescribed vertical profile $U_z(z) = U_{\text{out}}\Phi(\zeta)$ with $\Phi(1) = 1$, $\Phi(0) = 0$ [Eq. (5)], ensuring purely vertical issue at $z = H$ and vanishing axial speed at the floor.
- The impingement pedestal Δp_{imp} and turning loss K_{turn} [Eq. (6)], setting the near-floor static build-up.
- The composite rim pressure $p_{\text{edge}}(z)$ with shape $g(\zeta)$ [Eq. (8)] and cap $p_0 + \Delta P$.
- Initialization of the radial wall-jet at the turning radius r_t via (q, m) conditions in Eq. (11), then integral advancement using entrainment E, friction C_f and thickness growth $\delta'(r) = k_e$.

2.2 Core cushion model With $p_{\text{edge}}(z)$ now available, the core model solves:

$$\frac{1}{r}\,\partial_r\Big(r\,\rho\,\kappa_r\,\partial_r p\Big) + \partial_z\Big(\rho\,\kappa_z\,\partial_z p\Big) = 0, \quad \rho = \frac{p}{R_g\,T_\infty},$$

together with the Darcy-Stokes closure:

$$u = -\frac{\kappa_r}{\mu}\,\partial_r p, \qquad w = -\frac{\kappa_z}{\mu}\,\partial_z p,$$

where $\kappa_r = \alpha_r\,h^2$, $\kappa_z = \alpha_z\,h^2$. Boundary conditions:

- $\partial_r p(0, z) = 0$ (axis symmetry),
- $\partial_z p(r, 0) = \partial_z p(r, h) = 0$ (no-normal-flow at ground and disc surface),
- Mixed Robin sealing condition at $r = R^-$:

$$-\,\rho\,\kappa_r\,\partial_r p\big|_{r=R^-} = C_{\text{seal}}(z)\,[\,p(R^-, z) - p_0\,],$$

where $C_{\text{seal}}(z) = \chi\,(\rho_j U_z(z)^2/\mu)(b/H)(1/D_{m,\min})$ includes an empirical factor $\chi \in [0, 1]$ accounting for ground roughness and non-ideal sealing.

From the computed fields $p(r,z)$, $u(r,z)$, $w(r,z)$, the following integrated quantities are evaluated:

- Average cushion pressure: $\bar{p}_{\mathrm{core}} = \frac{1}{\pi (R^-)^2 h} \int_0^{R^-} \int_0^h p(r,z)\, 2\pi r \, dz \, dr$.
- Leakage mass flow through the peripheral ring: $\dot{m}_{\mathrm{leak}} = \int_{R^-}^{R_{\mathrm{tot}}} \int_0^h \rho(r,z)\, u(r,z)\, dz\, dr$ (or a suitably reduced one-dimensional approximation).
- Lift force: $L = \int_0^{R^-} (p(r,z) - p_0)\, 2\pi r \, dr \approx W$.

3. Iterative coupling and convergence

The overall algorithm proceeds as follows:

1. Choose an initial guess for U_{out}, $\dot{m}_{\mathrm{out}}$ and model parameters $(K_{\mathrm{turn}}, D_{m,\mathrm{min}}, E, C_f, k_e, m, \beta)$.
2. Build the curtain profile $U_z(z) = U_{\mathrm{out}} \Phi(\zeta)$ and the composite rim pressure $p_{\mathrm{edge}}(z)$ [Eqs. (5)–(8)].
3. Compute the sealing conductance $C_{\mathrm{seal}}(\zeta)$ and impose the Robin coupling at $r = R^-$ [Eq. (10)]; solve the core (Darcy–Brinkman) for $p(r,z), u, w$.
4. Initialize and march the radial wall-jet from r_t using (q,m) balances and $\delta'(r) = k_e$ to validate the near-floor behaviour.
5. Update $\bar{p}_{\mathrm{core}}$, $\dot{m}_{\mathrm{leak}}$, and lift L; enforce mass balance $\dot{m}_{\mathrm{in}} = \dot{m}_{\mathrm{out}} + \dot{m}_{\mathrm{leak}}$.
6. Check convergence on load, mass balance *and* a recirculation indicator (mean sign of u in a thin ring at $r \lesssim R^-$): if not converged, under-relax U_{out} and the pedestal weight via m in $g(\zeta)$, then repeat.

Convergence tolerances are typically $\varepsilon_L = \varepsilon_m = 10^{-3}$ and a rim-pressure update residual $\varepsilon_p = 10^{-4}$ (max-norm over $z \in [0,h]$). The under-relaxed update of U_{out} reads

$$U_{\mathrm{out}}^{(k+1)} = \omega\, U_{\mathrm{out}}^{(k)} + (1-\omega)\, U_{\mathrm{out}}^{\mathrm{target}}, \quad 0 < \omega < 1,$$

with $\omega \simeq 0.5$; a similar under-relaxation is applied to the exponent m in $g(\zeta)$.

Listing 1 – Solver outline (code-ready)

```
Given W, R_tot, h (=H), air props, alpha_r, alpha_z, b0, Dm_min, E, C_f, k_e:
  init U_out, mdot_out
  repeat
    # Curtain rim pressure (sealing BC)
    build U_z(z) = U_out * Phi(z/H)
    compute p_edge(z) with impingement + momentum sealing; cap at p0 + dP

    # Core solve (Darcy / Darcy-Brinkman)
    solve for p(r,z) with Robin at r=R_minus and no-normal-flow at z=0,h
    recover u, w from gradients

    # Mass & lift
    eval mdot_leak, L, and residuals:
      e_L = |L - W| / W
      e_m = |mdot_in - (mdot_out + mdot_leak)| / mdot_in

    # Wall-jet (consistency check)
    init q(rt), m(rt) and march with entrainment E, growth k_e, friction C_f

    # Update
    U_out = omega * U_out + (1 - omega) * U_out_target   (omega ~ 0.5)
  until (e_L < 1e-3) and (e_m < 1e-3) and rim-pressure residual < 1e-4
```

4. Outputs and interpretation

When the iterative loop has converged to a self-consistent state, the simulation returns:

- The core fields $p(r, z)$, $u(r, z)$, $w(r, z)$ and the derived out-of-plane vorticity $\omega_\theta = \partial_r w - \partial_z u$ to visualize the near-rim recirculation cell.
- The rim-pressure profile $p_{\text{edge}}(z)$, the sealing conductance $C_{\text{seal}}(\zeta)$, and the wall-jet integral quantities (entrainment, wall-jet speed/thickness evolution).
- The mass flows $\dot{m}_{\text{out}}$, $\dot{m}_{\text{leak}}$, and effective lift L, with the mass balance check $\dot{m}_{\text{in}} = \dot{m}_{\text{out}} + \dot{m}_{\text{leak}}$.
- The estimated outer-jet power $\dot{W}_{\text{jet}} \approx \dot{m}_{\text{out}} \frac{1}{2} U_{\text{out}}^2$ corrected by turning/impingement losses.
- A parameter-sensitivity summary for h, sealing performance and lift versus U_{out}, b_0, α_r, α_z, $D_{m,\min}$, E, C_f, k_e, m, β.

Diagnostic plots should include $U_z(z)$ and $p_{\text{edge}}(z)$ at $r = R^-$, and the sign of the radial velocity in a thin ring inside the rim.

4 Validity of Modeling Assumptions

4.1 Low-Mach Compressibility

The jets have typical velocities $U_{\text{out}} \approx 30$–$60\,\text{m/s}$, leading to a Mach number $Ma = U/a \approx 0.1$–0.2 with $a \simeq 343\,\text{m/s}$. This regime justifies a *low-Mach* formulation: the flow is compressible enough to exhibit pressure- and temperature-dependent density, but acoustic effects remain negligible. Hence, the ideal-gas relation $p = \rho R_g T$ is retained, while the flow is assumed quasi-static in time.

4.2 Thermal Uniformity and Energy Exchange

Although the confined air experiences some compression heating, the characteristic time scales of thermal diffusion and convective mixing by the curtain are short compared to global unsteadiness. The first-order model therefore assumes a uniform temperature $T = T_\infty$, with the understanding that future extensions may include the steady energy balance to recover small deviations of $T(r, z)$.

4.3 Stokes–Darcy Closure

The Stokes–Darcy model does not imply a porous medium in the literal sense. Instead, it approximates the momentum balance of a low-Reynolds, highly dissipative, confined flow. At low $Re = \rho U h/\mu$, the Stokes equations reduce to a linear proportionality between pressure gradient and velocity. Replacing $\nabla^2 \mathbf{u} \sim \mathbf{u}/L^2$ with an effective geometric length $L \sim h$ yields

$$\mathbf{u} \approx -\frac{h^2}{\mu}\nabla p, \tag{3}$$

which is mathematically equivalent to Darcy's law with an effective permeability $\kappa \sim h^2$. The anisotropic form used here,

$$\kappa_r = \alpha_r h^2, \qquad \kappa_z = \alpha_z h^2, \tag{4}$$

accounts for different confinement levels in the radial and vertical directions.

Validity range. This closure is valid provided that:

- the Reynolds number in the cushion $Re_c = \rho U_c h/\mu \ll 1$;
- pressure variations are slow and inertia negligible;
- the flow is quasi-steady and dominated by viscous losses and boundary friction;
- local turbulence and recirculation effects are absorbed into the empirical coefficients α_r, α_z.

It is particularly suited to parametric design and control studies where the detailed jet microstructure is not resolved.

4.4 Boundary Conditions and Curtain Coupling

The outer annular jet issues *downwards* and acts as an *air curtain* that limits radial leakage from the cushion. To enforce the requested kinematics — purely vertical at the injection plane and vanishing axial speed at the floor — we prescribe a smooth vertical profile for the curtain axial velocity:

$$U_z(z) = U_{\text{out}}\,\Phi(\zeta)\,, \qquad \zeta = \frac{z}{H}, \quad \Phi(1) = 1,\ \Phi(0) = 0, \tag{5}$$

with e.g. $\Phi(\zeta) = \sin^2\!\big(\frac{\pi}{2}\zeta\big)$ or $\Phi(\zeta) = \zeta^n$ ($n = 2$–3) to avoid cusps. This choice regularizes the turning of the curtain into a radial wall-jet along the ground.

Composite rim pressure with impingement pedestal. Upon impingement on the rigid floor, part of the curtain's kinetic energy is converted into static pressure. We model the impingement-induced pedestal as

$$\Delta p_{\text{imp}} = \xi_{\text{imp}}\,\frac{1}{2}\,\rho_j\,U_{\text{out}}^2, \qquad \xi_{\text{imp}} = \frac{1}{1 + K_{\text{turn}}}, \tag{6}$$

where K_{turn} is a turning-loss coefficient. The rim pressure along $r = R^-$ is then defined by a composite (pedestal + momentum-sealing) expression, capped by the available head ΔP:

$$p_{\text{edge}}(z) = p_0 + \underbrace{\Delta p_{\text{imp}}\, g(\zeta)}_{\text{impingement pedestal}} + \underbrace{\left(\frac{\rho_j\, U_z(z)^2\, b(z)}{H}\right) \frac{1}{D_{m,\min}}\, [1 - g(\zeta)]}_{\text{momentum sealing}} \tag{7}$$

with

$$p_{\text{edge}}(z) \le p_0 + \Delta P. \tag{8}$$

Here $g(\zeta)$ is a monotone increasing shape (e.g. $g(\zeta) = 1-(1-\zeta)^m$, $m \in [2,4]$) that shifts weight from momentum sealing aloft to static build-up near the floor. The effective slot width may be taken as $b(z) = b_0 + s\, z$ to reflect geometric spreading.

Physical consistency. The rim pressure must satisfy $p_{\text{edge}}(z) \ge p_0$. Moreover, the curtain work over the near-floor seal strip should be commensurate with the injected momentum flux, e.g.

$$\int_0^h [p_{\text{edge}}(z) - p_0]\, \mathrm{d}z \;\sim\; \mathcal{O}\left(\frac{\rho_j U_{\text{out}}^2\, b_0}{D_{m,\min}}\right), \tag{9}$$

which prevents non-physical rim over-pressurization in the coupling.

Robin sealing condition at the rim. Instead of prescribing $p(R^-, z) = p_{\text{edge}}(z)$ (pure Dirichlet), we impose a mixed *Robin* condition that filters the exchange through the curtain, consistent with its local momentum:

$$-\rho\, \kappa_r\, \partial_r p\big|_{r=R^-} = C_{\text{seal}}(\zeta)\, (p(R^-, z) - p_0), \qquad C_{\text{seal}}(\zeta) = \frac{\rho_j\, U_z(z)^2}{\mu}\, \frac{b(z)}{H}\, \frac{1}{D_{m,\min}}\, [1 - g(\zeta)]. \tag{10}$$

This promotes a realistic near-floor recirculation: the curtain pushes air downward and radially outward at the ground, while the low-ζ reduction of C_{seal} limits leakage and bends streamlines back into the core.

Wall-jet initialization at the turning radius. At the ground ($z = 0$), in the narrow annulus where the curtain turns radially, we initialize the radial wall-jet with thickness δ_t and characteristic speed $U_c(r_t)$ at the turning radius r_t by continuity of mass and momentum (including K_{turn}):

$$q(r_t) = \rho\, U_c(r_t)\, \delta_t, \qquad m(r_t) = \rho\, U_c(r_t)^2\, \delta_t. \tag{11}$$

Downstream, the wall-jet integral balances are advanced with entrainment E and skin-friction C_f as in the base model.

5 Non-dimensional formulation

To improve the clarity and scalability of the numerical results, all quantities are expressed in non-dimensional form using characteristic reference scales of the system. The aim is to identify the dominant parameters governing both the pressure field in the inner core and the performance of the outer jet curtain.

5.1 Reference quantities

Let R_{tot} denote the total radius of the levitating disk and h the nominal hovering height. The characteristic velocity and pressure are defined as:

$$U_c = \frac{\kappa_r \, p_c}{\mu \, R_{\mathrm{tot}}}, \qquad p_c = \frac{W}{\pi R_{\mathrm{tot}}^2},$$

where p_c represents the mean cushion pressure required to support the total load W, κ_r the effective radial permeability, and μ the dynamic viscosity of air.

Density and temperature are normalized with respect to their ambient values, ρ_0 and T_0, respectively.

5.2 Dimensionless variables

The spatial coordinates, velocity components, pressure and density are expressed as:

$$\hat{r} = \frac{r}{R_{\mathrm{tot}}}, \qquad \hat{z} = \frac{z}{h}, \qquad \hat{u} = \frac{u}{U_c}, \qquad \hat{w} = \frac{w}{U_c \, h/R_{\mathrm{tot}}}, \qquad \hat{p} = \frac{p - p_0}{p_c}, \qquad \hat{\rho} = \frac{\rho}{\rho_0}.$$

Here p_0 is the ambient static pressure outside the flow domain. The scaling of w accounts for the typical geometric aspect ratio of the system, where vertical velocities are smaller by a factor of h/R_{tot}.

5.3 Governing equations in dimensionless form

Substituting the above definitions into the Darcy-like formulation for the core region yields:

$$\hat{u} = -\hat{\kappa}_r \frac{\partial \hat{p}}{\partial \hat{r}}, \qquad \hat{w} = -\hat{\kappa}_z \frac{\partial \hat{p}}{\partial \hat{z}},$$

$$\frac{1}{\hat{r}} \frac{\partial}{\partial \hat{r}} \left(\hat{r} \, \hat{\rho} \, \hat{u} \right) + \frac{R_{\mathrm{tot}}}{h} \frac{\partial}{\partial \hat{z}} \left(\hat{\rho} \, \hat{w} \right) = 0,$$

with the non-dimensional permeability ratios

$$\hat{\kappa}_r = \frac{\kappa_r}{\kappa_r^0}, \qquad \hat{\kappa}_z = \frac{\kappa_z}{\kappa_r^0},$$

and an anisotropy parameter

$$S = \frac{\kappa_z}{\kappa_r} \frac{R_{\mathrm{tot}}}{h},$$

which quantifies the degree of preferential flow direction within the core.

The ideal-gas equation of state becomes

$$\hat{p} + \frac{p_0}{p_c} = \frac{\rho_0 R_g T_0}{p_c} \, \hat{\rho} \, \frac{T}{T_0},$$

and, under the isothermal assumption $T = T_0$, simplifies to $\hat{p} = (p/p_c) - (p_0/p_c) = (\rho/\rho_0) - (p_0/p_c)$.

5.4 Dimensionless groups

The flow behaviour in the cushion region can be characterized by a small number of non-dimensional parameters:

$$\mathrm{Re} = \frac{\rho_0 U_c R_{\mathrm{tot}}}{\mu}, \qquad \mathrm{Ma} = \frac{U_c}{a_0}, \qquad \Gamma = \frac{h}{R_{\mathrm{tot}}}, \qquad S = \frac{\kappa_z}{\kappa_r} \frac{R_{\mathrm{tot}}}{h},$$

where Re and Ma are the Reynolds and Mach numbers respectively, and Γ the geometric aspect ratio. A key design group is the *seal number*

$$\Sigma \;=\; \frac{\rho_j U_{\text{out}}^2\, b}{H\, p_c}, \tag{12}$$

which measures the dynamic capacity of the curtain relative to the cushion pressure. Values $\Sigma \gtrsim 3$–5 are typically required for robust sealing at moderate gaps.

5.5 Non-dimensionalization of the outer jet

For the outer annular jet, the characteristic scales are based on its inlet velocity U_j, slit width b, and density ρ_j. Dimensionless quantities are defined as:

$$\hat{r}_j = \frac{r - R^-}{b}, \qquad \hat{z}_j = \frac{z - h}{b}, \qquad \hat{U} = \frac{U}{U_j}, \qquad \hat{p}_j = \frac{p - p_0}{\rho_j U_j^2}.$$

The corresponding Reynolds number and pressure coefficient are:

$$\text{Re}_j = \frac{\rho_j U_j b}{\mu}, \qquad C_p = \frac{p - p_0}{\frac{1}{2}\rho_j U_j^2}.$$

The non-dimensional entrainment and wall-friction effects are represented by:

$$E^* = \frac{E}{U_j}, \qquad C_f^* = C_f \frac{R_{\text{tot}}}{b},$$

while the turn-loss and minimum-momentum-deflection parameters are introduced as:

$$K_{\text{turn}}^* = \frac{K_{\text{turn}}}{\rho_j U_j^2}, \qquad D_{m,\min}^* = D_{m,\min}.$$

This formulation allows direct comparison between the dynamic capacity of the jet ($\rho_j U_j^2 b/H$) and the dimensionless cushion pressure $\hat{p}_c = p_c/(\rho_j U_j^2)$, thereby linking the jet operating point with the pressure sustained in the core.

5.6 Interpretation

With this formulation: - quantities inside the core scale naturally with the load W, geometry (R_{tot}, h), and permeability ratios; - quantities related to the outer jet scale with its momentum flux and geometric confinement parameters (b, H); - the coupling condition at the interface $r = R^-$ can be expressed consistently as a non-dimensional pressure continuity constraint:

$$\hat{p}_{\text{edge}} \;=\; \min\!\left(\frac{\Delta P}{p_c},\; \frac{\Sigma}{D_{m,\min}}\right).$$

ensuring that both regions share a unified, dimensionless reference frame.

6 Simulation Outputs

The results produced from the model are shown in this section.

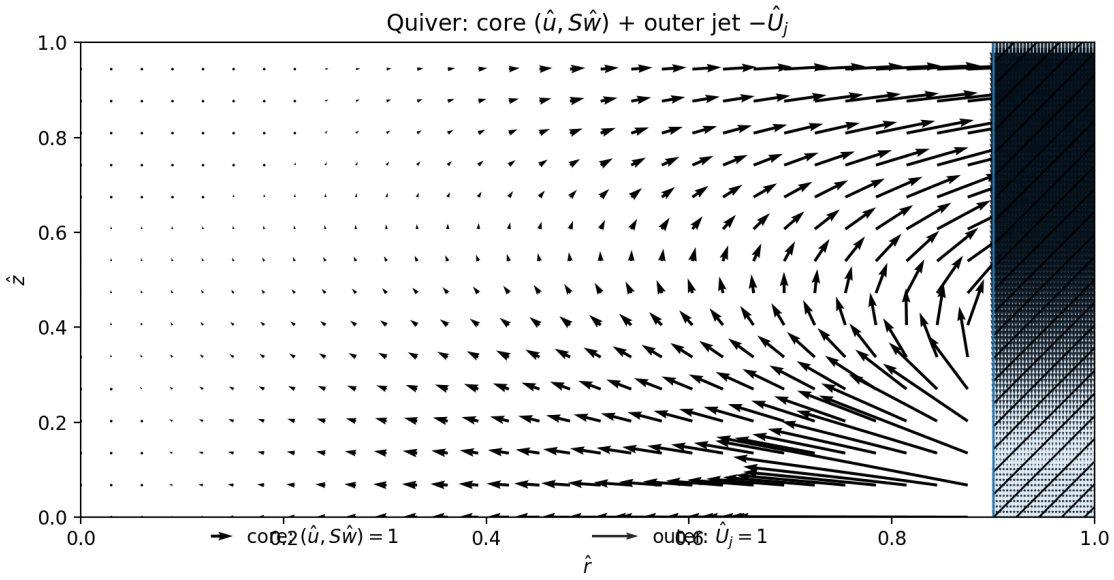

Figure 2 – Non-dimensional velocity field (quiver). Vectors show $(\hat{u},\, S\hat{w})$ for isotropic visual scaling; the pattern reflects the rim-imposed sealing pressure from the downward curtain.

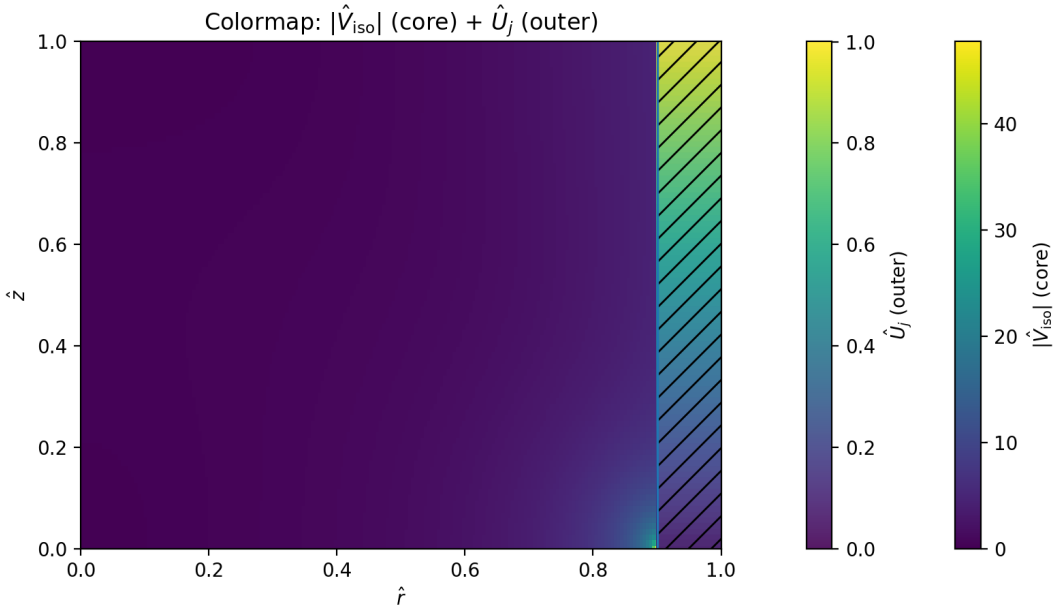

Figure 3 – Colormap of the non-dimensional isotropic speed magnitude $\hat{V}_{\text{iso}} = \sqrt{\hat{u}^{\,2} + S^2\hat{w}^{\,2}}$.

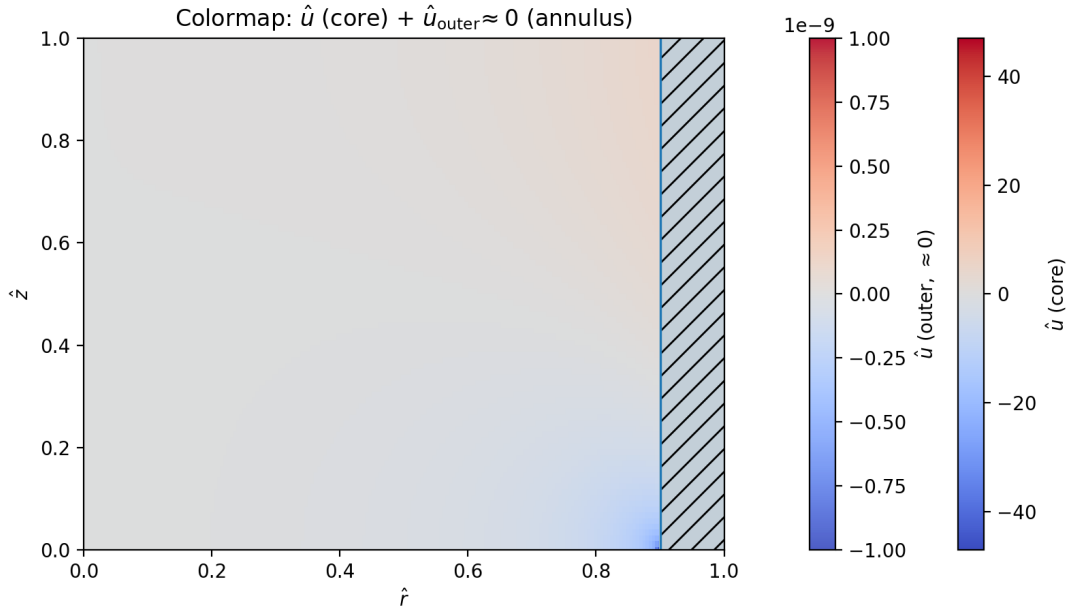

Figure 4 – Colormap of the non-dimensional radial component magnitude $|\hat{u}|$.

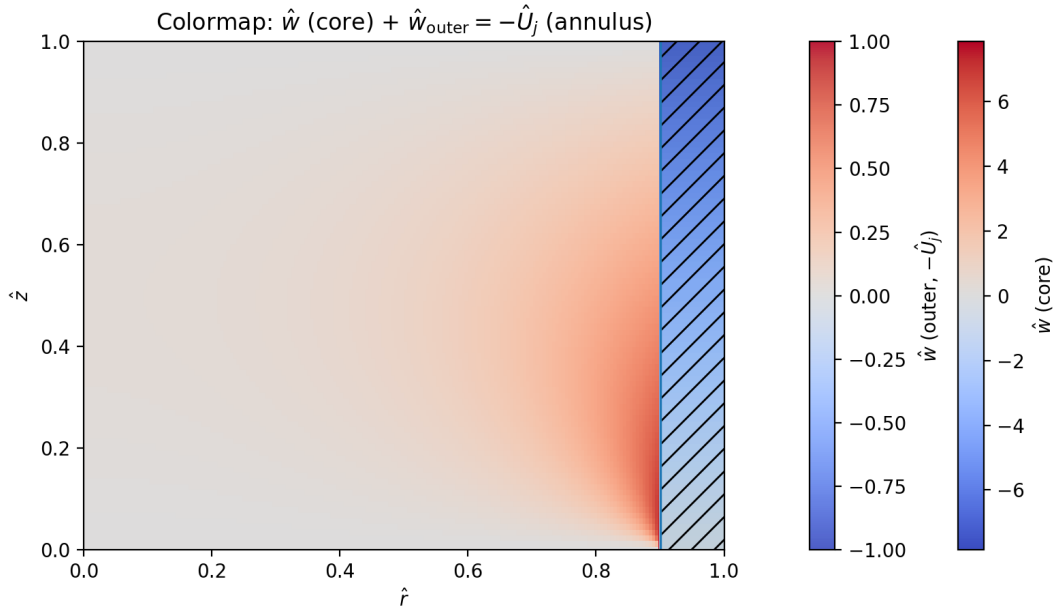

Figure 5 – Colormap of the non-dimensional axial component magnitude $|\hat{w}|$.

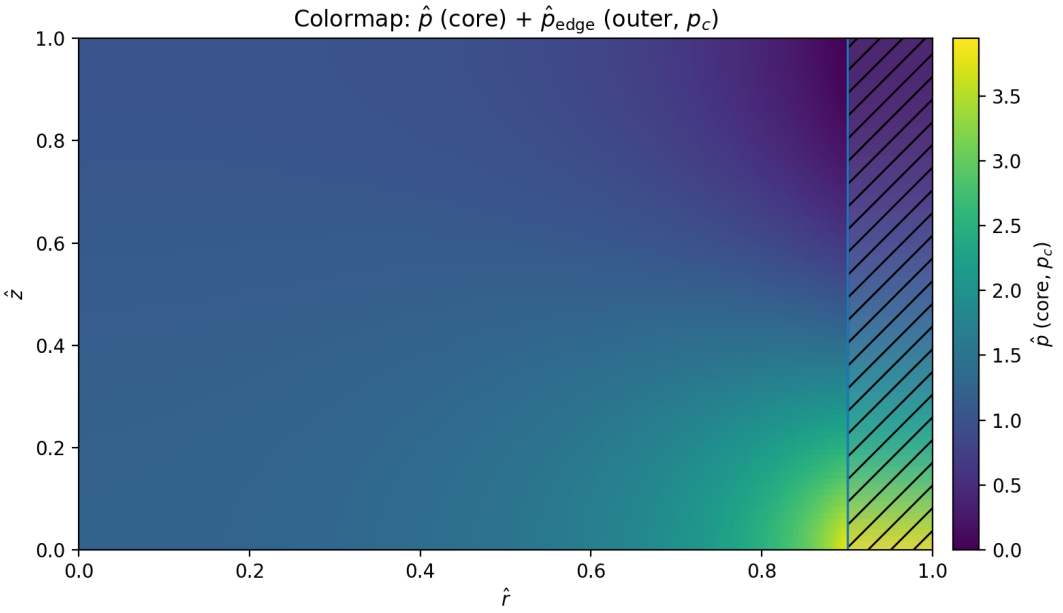

Figure 6 – Colormap of the non-dimensional pressure $\hat{p}$.

Performance and stability analysis. From the converged solutions the lift–height characteristic $L(h)$ is evaluated to assess static stability. A stable hovering point satisfies $dL/dh < 0$ in the neighbourhood of the nominal gap. The required jet power is estimated as

$$\dot{W}_{\text{jet}} = \frac{1}{2}\dot{m}_{\text{out}} U_{\text{out}}^2/(1 + K_{\text{turn}}),$$

and the non-dimensional sealing and leakage indices are

$$\Pi_{\text{seal}} = \frac{\rho_j U_{\text{out}}^2 b}{H p_c}, \qquad \Pi_{\text{leak}} = \frac{\dot{m}_{\text{leak}}}{\rho_0 U_{\text{out}} 2\pi R^- b}.$$

Together with the seal number Σ and the efficiency η, these provide quick performance metrics for design optimization. A convenient energetic metric is the sealing efficiency,

$$\eta \;=\; \frac{W\,h}{\dot{W}_{\text{jet}}},$$

which grows with improved sealing (lower leakage for a given $\dot{W}_{\text{jet}}$).

Design Procedure Summary

1. Specify W, R, h, and air properties (ρ_0, μ, T_0).
2. Compute target cushion pressure $p_c = W/(\pi R^2)$.
3. Choose seal number target $\Sigma_{\min} \in [3, 5]$ and estimate $U_{\text{out}} = \sqrt{\Sigma_{\min} H p_c/(\rho_j b)}$.
4. Evaluate Ma, Re_j and adjust (b, H) for $Ma < 0.3$, $Re_j > 2000$.
5. Iterate the coupled solver until $|L - W|/W < 10^{-3}$ and mass balance error $< 10^{-3}$.
6. Output: $L(h)$ curve, Π_{seal}, Π_{leak}, $\dot{W}_{\text{jet}}$.

7 Model Limitations and Planned Extensions

The present formulation uses the Darcy–Brinkman reduction as an effective description of the viscous core. Coefficients α_r and α_z should be calibrated from axisymmetric CFD or experiments. The secondary make-up flow is lumped into the global mass balance rather than as a local inlet. Thermal effects are neglected ($T = T_\infty$) and Mach numbers remain below 0.3. Future extensions will introduce a steady energy equation, refined wall-jet correlations and the automated lift-matching loop. Potential unsteady feedback (vertical oscillations) may arise from the coupling between cushion compressibility and curtain dynamics; this can be assessed by linearizing the mass balance around the hovering point to check that $dL/dh < 0$ and adding a simple lumped compliance model for the core.

Appendix: minimal rationale for the composite rim pressure. Consider a control volume hugging the rim over height h and thickness $O(b)$. A downward slot jet of density ρ_j and speed U_{out} is deflected into a radial wall-jet of speed $U_r(z)$ near the floor. A crude momentum balance suggests a static build-up $\Delta p_{\text{stat}} \sim \rho_j U_{\text{out}}^2\, \mathcal{O}(1)$ concentrated near $\zeta \to 0$, while the resistance to cross-flow (sealing) scales with the jet momentum flux impinging near the slot, $\Delta p_{\text{seal}} \sim \rho_j U_{\text{out}}^2\, \mathcal{O}(1)$ for $\zeta \to 1$. The composite form $\rho_j U_{\text{out}}^2\, [\, C_p(1-\zeta)^n + C_s \zeta^m \,]$ is thus a first-order surrogate capturing both effects with two tunable, dimensionless coefficients (C_p, C_s) and mild shape exponents (m, n).

On the choice of $D_{m,\min}$. We take $D_{m,\min}$ from air-curtain literature (order 10^{-1}) as a design parameter; in absence of calibration, $D_{m,\min} = 0.2$ provides a conservative default. Sensitivity to this parameter should be reported alongside calibrated runs.

8 Nomenclature

Symbol	Description
R_{tot}	Total radius of the disc
R^-	Inner radius of the leakage ring (centreline of jet slot, $R^- = R_{\text{tot}} - b_0/2$)
h	Hovering height (disc–ground gap)
h_{eff}	Effective sealing height at rim
b_0	Slot thickness at injection (plane jet width)
$b(z)$	effective local width of the curtain slot or equivalent jet region as a function of z
U_{out}	Outer jet velocity
ρ_j	Density of outer jet
ρ	Density in the core region
p, p_0, p_c	Local, ambient, and cushion pressures
T, T_∞	Local and ambient temperatures
μ	Dynamic viscosity of air
R_g	Specific gas constant of air
W	Payload supported by cushion
κ_r, κ_z	Effective permeabilities (radial/axial)
α_r, α_z	Dimensionless permeability coefficients
u, w	Velocity components (radial, vertical)
Δp	Rim pressure increment
$\mathcal{A}$	Permeability anisotropy parameter
$\hat{r}, \hat{z}, \hat{p}$	Dimensionless coordinates and pressure
$\hat{u}, \hat{w}$	Dimensionless velocity components
S	Velocity anisotropy ratio $S = (\alpha_z/\alpha_r)(R_{\text{tot}}/h)$
D_m	Deflection modulus (momentum index) $\rho U_0^2 b_0/(\Delta P\, H)$
Σ	Seal number $\Sigma = \rho_j U_{\text{out}}^2 b/(H p_c)$
η	Sealing efficiency $\eta = Wh/\dot{W}_{\text{jet}}$
$D_{m,\min}$	Minimum deflection modulus for sealing
H	Effective curtain height
s	Jet spreading parameter (≈ 0.06–0.09)
$\Delta P_{\max}$	Maximum sustainable pressure difference
$q(r)$	Mass flow per unit circumference in wall-jet model
$m(r)$	Momentum flux per unit circumference in wall-jet model
δ_t	Wall-jet thickness at turning radius r_t
r_t	Effective turning radius of the outer jet on the ground
$U_c(r)$	Local characteristic velocity of the wall-jet at radius r

Additional symbols.

r_t	effective turning radius of the outer jet
U_{out}	injection speed of the outer (vertical) jet
A_{slot}	outlet area of the outer jet
K_{turn}	momentum loss coefficient at turning (impingement)
δ, δ_t, δ_s	wall-jet thickness (generic / at r_t / at r_-)
$U_c(r)$	characteristic wall-jet speed
$q(r)$, $m(r)$	mass and momentum per unit circumference
E	entrainment coefficient
C_f	wall friction coefficient, $C_f = C_{f0} Re_\delta^{-1/5}$
k_e	wall-jet thickness growth rate
w_s	seal strip width, $w_s = \lambda\, \delta_s$
δ_p	effective thickness for pressure work in the seal strip
Δp	pressure jump between core and ambient